Inorganica Chimica Acta 392 (2012) 221–228

Contents lists available at SciVerse ScienceDirect

Inorganica Chimica Acta

journal homepage: www.elsevier.com/locate/ica

Binuclear cobalt complex with Schiff base ligand: Synthesis, characterization and catalytic properties in partial oxidation of cyclohexane

Liudmila I. Rodionova [a,*], Andrey V. Smirnov [a], Natalya E. Borisova [a], Victor N. Khrustalev [b], Anna A. Moiseeva [a], Wolfgang Grünert [c]

[a] Department of Chemistry, Lomonosov Moscow State University, Lenin Hills 1/3, 119991 Moscow, Russian Federation
[b] A.N. Nesmeyanov Institute of Organoelement Compounds, Russian Academy of Sciences, Vavilov Street 28, 119991 Moscow, Russian Federation
[c] Ruhr-Universität Bochum, P.O. Box 10 21 48, D-44801 Bochum, Germany

ARTICLE INFO

Article history:
Received 16 March 2012
Received in revised form 31 May 2012
Accepted 1 June 2012
Available online 19 June 2012

Keywords:
Cyclohexane oxidation
Binuclear cobalt complex
Schiff bases

ABSTRACT

A new binuclear cobalt complex with Schiff base ligand and amino acid was synthesized and characterized using XRD, elemental analysis, IR spectroscopy, XPS and electrochemical measurements. The presence of cobalt in the oxidation state 3+ in this complex was proved. The catalytic activity of this complex was investigated in the reaction of partial cyclohexane oxidation with air, and high activity and selectivity for cyclohexanol and cyclohexanone formation were demonstrated. The possibility of complex reuse in cyclohexane oxidation was studied and it was shown that the activity slightly decreases in a second oxidation cycle along with changes in main product distribution due to partial transfer of Co^{3+} to Co^{2+}.

1. Introduction

One of the most promising directions of petroleum hydrocarbon feedstock conversion is its partial oxidation with air to valuable products [1]. Among these processes, the catalytic oxidation of cyclohexane to a mixture of cyclohexanol and cyclohexanone becomes increasingly important due to great need of these products as precursors in caprolactam and Nylon-6 synthesis [2]. One of the first industrial alkane oxidation processes – the Du Pont adipic acid process [3], which involves homogeneous cyclohexane oxidation with air on cobalt salts, such as naphthenate or acetate, initiated an intense research activity devoted to catalytic cyclohexane oxidation over heterogeneous and homogeneous cobalt systems [4–10] using different oxidants such as air [5,6], pure oxygen [7], hydrogen peroxide [8,9] and organic hydroperoxides [10].

As cyclohexanol and cyclohexanone are more easily oxidized than the initial cyclohexane, conversion is kept at low levels (about 4–5%) to avoid the formation of side products by deeper oxidation of the cyclohexanol–cyclohexanone mixture [3]. In this connection, it is of prime importance to find new catalysts which selectively oxidize only cyclohexane.

Mono- and binuclear complexes of transitional metals with Schiff base ligands attract attention since they are structural and composition analogs of some biological active compounds [11]. Many researchers are focused on producing systems which can mimic not only structural but also catalytic properties of metalloenzymes [12–15]. Based on such biological processes as methane oxidation on monooxygenase [12,13,15] or steroids oxidation on cytochrome P450 [14], new complexes for catalytic oxidation of alkanes, olefins, alcohols and aldehydes are being developed.

The detailed study of structure, state of metal and catalytic activity of such complexes can result the in elucidation of the mechanisms of biocatalyzed oxidation processes.

In this article a binuclear cobalt complex **CoL** with Schiff base ligand and L-valine will be described. The composition and structure of this complex were characterized by IR spectroscopy, elemental analysis, XRD, XPS and electrochemical measurements. The complex was tested in cyclohexane oxidation with air and showed high activity and selectivity to the cyclohexanol–cyclohexanone mixture.

2. Experimental

2.1. Synthesis

2.1.1. Synthesis of sodium salt of the ligand (see Scheme 2)

To the solution of 115 mg (5 mmol) of Na in anhydrous methanol (30 ml) 590 mg (5 mmol) of solid L-valine was added and the mixture was stirred until complete dissolution. After the addition of the equimolar amount of 5-chloro-2-hydroxy-3-nitrobenzaldehyde (5 mmol) the mixture was stirred for 3 h at room temperature and a dark crimson solution was formed. After evaporation of this solution, a dark red product was formed.

* Corresponding author. Tel.: +7 (495) 939 2054; fax: +7 (495) 939 3570.
E-mail address: ludmilarodionova@mail.ru (L.I. Rodionova).

0020-1693/$ - see front matter © 2012 Elsevier B.V. All rights reserved.
http://dx.doi.org/10.1016/j.ica.2012.06.017

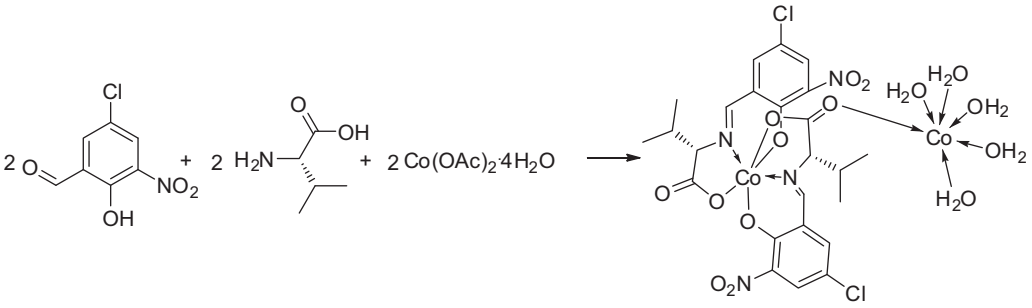

Scheme 1.

Anal. Calc. for $C_{12}H_{12}ClNaN_2O_5$: C, 44.67; N, 8.68; H, 3.75; Na, 7.22. Found: C, 44.5; N, 8.92; H, 3.63; Na, 6.94%. IR (KBr, cm^{-1}): 3427, 2965, 2929, 2862, 1648, 1609, 1534, 1510, 1398, 1340, 1280, 1221. ^1H NMR (400 MHz, methanol-d_4) δ ppm 1.02 (t, J = 6.85 Hz, 6 H) 2.40 (tq, J = 6.60, 5.26 Hz, 1 H) 3.98 (br, s, 1 H) 7.67 (d, J = 2.93 Hz, 1 H) 7.90 (s, 1 H) 8.11 (d, J = 2.69 Hz, 1 H) 8.48 (s, 1 H).

2.1.2. Synthesis of complex [16] (Scheme 1)

5-Chloro-2-hydroxy-3-nitrobenzaldehyde 1 g (5 mmol) and 590 mg (5 mmol) of L-valine were dissolved in 50 ml of an ethanol–water (3/1) mixture and heated for 2 h. After this period, 1.254 g (5 mmol) of solid cobalt(II) acetate tetrahydrate was added and the mixture was diluted with 50 ml of water and sonicated for 10 min to avoid precipitation of unreacted cobalt salt. The reaction mixture was filtered, washed with water and diethyl ether. The collected solid was air dried overnight and then over NaOH in a desiccator, whereupon dark brown crystals were formed.

The substance thus formed was soluble in methanol and insoluble in diethyl ether and water. The structure of complex, denoted as **CoL**, was confirmed by IR spectroscopy and X-ray diffraction.

Anal. Calc. for $C_{24}H_{32}Cl_2Co_{1.5}N_4O_{15}$: C, 37.12; N, 7.22; H, 4.12; Co, 11.4; Found: C, 36.75; N, 6.98; H, 4.04; Co, 11.7. IR (KBr, cm^{-1}): 3376, 2967, 2929, 2862, 1647, 1597, 1533, 1515, 1438, 1383, 1354, 1315, 1287, 1228, 1197, 1135.

2.2. Physical measurements

The elemental analysis (carbon, hydrogen and nitrogen) of the complex was obtained by a Thermo Flash EA 1112 series analyzer. XPS (X-ray photoelectron spectroscopy) data were recorded with the Leyboldt LH 10/100, using Magnesium Kα excitation (1253.6 eV). The residual pressure in the spectrometer during the runs was about 10^{-8} Pa. The sample was vacuumized at liquid nitrogen temperature. The spectrometer energy scale was calibrated using Au 4f7/2 photoelectron line at 84.0 eV, the correction for surface charging was made by setting the C 1s signal of aromatic and aliphatic C to 284.5 eV. The metal content was measured using thermogravimetric analysis (TA Instruments, SDT Q600) in air flow by complex decomposition to constant mass, which was determined as Co_3O_4. FTIR spectra were recorded on a Nicolet Protege 460 spectrometer in KBr pellets.

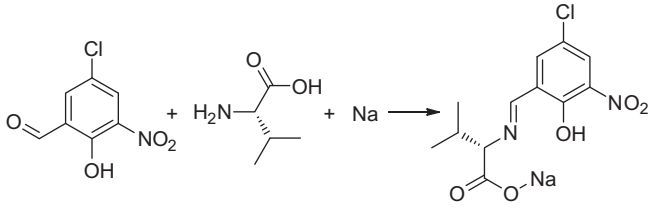

Scheme 2.

Electrochemical studies (cyclic voltammetry) were carried out on a IPC-Pro M potentiostat. A glassy-carbon disk with diameter of 2 mm was used as working electrode; a 0.1 M Bu_4NClO_4 (TBP) solution in DMF (high-purity grade) served as the supporting electrolyte; Ag/AgCl/KCl(satd.) was used as reference electrode and a platinum electrode as counter electrode. The sample concentration was 10^{-3} mol/l. All measurements were carried out under argon; the samples were dissolved in the deaerated solvent. The scan rate was 200 mV s^{-1}. All potentials are given taking into account IR-compensation.

2.2.1. X-ray crystal structure determination

A red prismatic crystal ($0.1 \times 0.1 \times 0.3$ mm^3) of **CoL** ($C_{24}H_{27}N_4O_{12.5}Cl_2Co_{1.5}\cdot 2.5H_2O$, M = 775.83) is trigonal, space group $P3_121$, at T = 100 K: a = 15.7626(9) Å, c = 24.8669(14) Å, V = 5350.7(5) $Å^3$, Z = 6, d_{calc} = 1.445 g/cm^3, $F(000)$ = 2391, μ = 0.923 mm^{-1}. A total of 51 478 reflections (7047 unique reflections, R_{int} = 0.065) were measured on a Bruker SMART APEX II CCD diffractometer (λ(Mo Kα)-radiation, graphite monochromator, ω and φ scan mode, $2\theta_{max}$ = 52°) and corrected for absorption using the SADABS program [17]. The structure was determined by direct methods and refined by a full-matrix least squares technique on F^2 with anisotropic displacement parameters for non-hydrogen atoms. The absolute structure of **CoL** was objectively determined by the refinement of Flack parameter, which has become equal to 0.03(3). The hydrogen atoms of the water molecules were localized in the difference-Fourier map and included in the refinement with fixed positional and isotropic displacement parameters. The other hydrogen atoms were placed in the calculated positions and refined within a riding model with fixed isotropic displacement parameters ($U_{iso}(H) = 1.5U_{eq}(C)$ for the CH_3-groups and $U_{iso}(H) = 1.2U_{eq}(C)$ for the other groups). The final divergence factors were R_1 = 0.080 for 5218 independent reflections with $I > 2\sigma(I)$ and wR_2 = 0.206 for all independent reflections, S = 1.007. All calculations were carried out using the SHELXTL program [18].

2.3. Cyclohexane oxidation

Cyclohexane (CyH) oxidation was carried out in a 100 ml stainless steel batch reactor equipped with a magnetic stirrer. In a typical experiment 0.36 mol of cyclohexane, 0.09 mol of toluene as internal standard and 6.5×10^{-6} mol of catalyst were added to the autoclave. The system was pressurized with air and then heated under permanent stirring. The operating temperature, measured by a thermocouple inside the reactor, was 140 °C. The operating pressure after heating was maintained at 25 atm. The main products, such as cyclohexanol (CyOH) and cyclohexanone (CyO), were analyzed by gas–liquid chromatography, cyclohexyl hydroperoxide (CyOOH) was detected by iodometric titration with

sodium thiosulfate, acids were analyzed by titration with NaOH, as describe in literature [19].

To determine the possibility to reuse of the **CoL** complex in cyclohexane oxidation, **CoL** was precipitated from products with water after the catalytic experiment, washed with water and acetone and tested in the catalytic oxidation of cyclohexane in a second cycle. The sample thus formed was denoted as re-used **CoL**.

3. Results and discussion

To synthesize new cobalt complex we lead the way proposed by Casella and Gullotti: we use the possibility of the template condensation of the aldehydes with amine in presence of metal salt [16]. The template rout toward the cobalt complexes with chiral azomethines based on L-valine amino acid is typical method [20–22]. The over used procedure for the preparation of the complexes with Schiff bases is reaction of the metal salt with the formerly prepared ligand, but this way is less popular and to the best of our knowledge this procedure never used for preparation of chiral compounds [23–30] probably due to racemization [31,32]. The 5-chloro-2-hydroxy-3-nitrobenzaldehyde reacts easily with L-valine and cobalt salt in anhydrous methanol at room temperature to form the binuclear cobalt complex **CoL** (Scheme 1) as a product of the template condensation.

For understanding the electrochemical behavior of the complex and for separation of the possible electrochemical activity of the ligand itself from the potentials of the metal ion-concentrated redox processes we need to compare the electrochemical behavior of the complex thus formed with its ligand. For this purpose the sodium salt of the corresponding Schiff base was synthesized according to Scheme 2 and was denoted as **NaL**.

3.1. X-ray diffraction study

Single crystals for X-ray diffraction were obtained from a CH_3OH solution. A representation of the X-ray structure is shown in Figs. 1 and 2 along with the atomic numbering scheme, and selected bond lengths and angles are listed in Table 1. The cationic $[Co(H_2O)_5]^{2+}$ fragment of **CoL** is disordered over two sites relative to the twofold axis. The crystal of **CoL** contains four water solvate molecules per complex. Three water solvate molecules are statistically disordered with the total positional occupancies of 0.5, one of which is also disordered over two sites in the ratio of 0.3:0.2.

The crystal structure of **CoL** is very similar to the related $[Co(H_2O)_6][Co(C_9H_7NO_3)_2]_2{\cdot}2H_2O$ (**CoL′**) [33] and $[Co(H_2O)_6][Co(C_9H_7NO_3)_2]_2{\cdot}H_2O$ (**CoL″**) [34]. The main difference between these structures is that **CoL** is one whole complex, whereas **CoL′** and **CoL″** are salts with separated cationic and anionic parts.

The Co(III) cobalt atom is six coordinate with a slightly distorted octahedron. The six coordination sites are occupied by four oxygen and two nitrogen atoms from two Schiff-base (salicylideneglycine) ligands. The Co1 cobalt atom lies within the O1–O3–O6–O8 basal plane and the N1 and N3 nitrogen atoms occupy the axial positions forming a N1–Co1–N3 angle of 170.9(2)°. Comparing the N–Co–N angles in **CoL**, **CoL′** (173.6(3)°) and **CoL″** (173.5(1)°), compound **CoL** is more distorted than the compounds **CoL′** and **CoL″**. The salicylideneglycine ligands are not planar. The six-membered metallocycles adopt a *sofa* conformation with the deviation of the Co1 atom from the plane through the other atoms of the cycles (0.817 and 0.656 Å, respectively), and the five-membered metallocycles adopt an *envelope* conformation with the deviation of the nitrogen atom from the plane through the other atoms of the cycles (0.310 and 0.339 Å, respectively). Thus, the each ligand can be described by two planes which are defined by their 5- and 6-membered rings. The intersection angles of these planes with each other (42.9° and 37.6°, respectively) indicate the buckled nature of the ligands.

The **CoL** compound possesses two asymmetric centers at the C2 and C14 carbon atoms with the absolute configurations of 2***S***,14***S***.

The Co(II) cobalt atom is octahedrally coordinated to one carbonyl and five hydrate oxygen atoms. The cationic $[Co(H_2O)_5]^{2+}$ fragment of the compound **CoL** is disordered over two sites relative

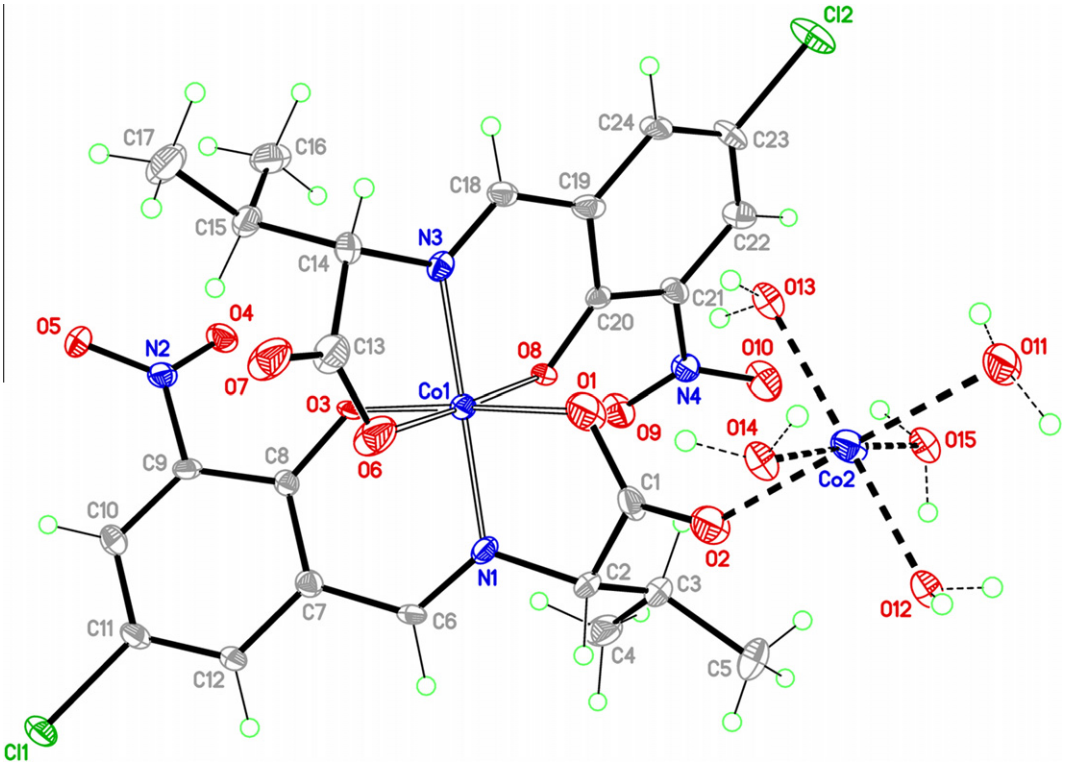

Fig. 1. X-ray structure of **CoL**. The disordered $[OCo(H_2O)_5]$ fragment is depicted by dashed lines. The solvate water molecules are not shown.

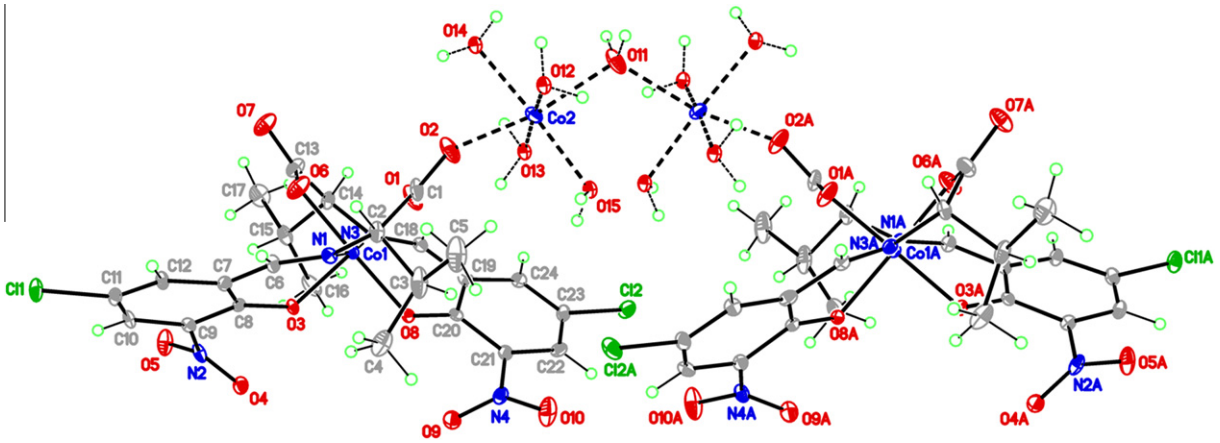

Fig. 2. A part of the crystal structure of **CoL** showing the disorder of the $[OCo(H_2O)_5]$ fragment relative to twofold axis.

Table 1
Selected bond lengths (Å) and angles (°) for **CoL**.

Co1–O1	1.906(4)	Co2–O2	2.016(5)
Co1–O3	1.892(3)	Co2–O11	2.201(4)
Co1–O6	1.895(4)	Co2–O12	1.949(9)
Co1–O8	1.902(3)	Co2–O13	2.078(9)
Co1–N1	1.896(5)	Co2–O14	2.045(8)
Co1–N3	1.879(5)	Co2–O15	2.098(8)
O1–Co1–O3	176.6(2)	O2–Co2–O11	169.8(2)
O1–Co1–O6	89.7(2)	O2–Co2–O12	90.5(3)
O1–Co1–O8	89.8(2)	O2–Co2–O13	87.8(3)
O3–Co1–O6	91.2(2)	O2–Co2–O14	76.4(3)
O3–Co1–O8	89.4(1)	O2–Co2–O15	99.6(3)
O6–Co1–O8	177.7(2)	O11–Co2–O12	86.7(2)
O1–Co1–N1	84.1(2)	O11–Co2–O13	95.7(2)
O3–Co1–N1	92.7(2)	O11–Co2–O14	93.8(3)
O6–Co1–N1	88.0(2)	O11–Co2–O15	90.0(3)
O8–Co1–N1	94.3(2)	O12–Co2–O13	175.3(3)
O1–Co1–N3	90.8(2)	O12–Co2–O14	91.9(3)
O3–Co1–N3	92.6(2)	O12–Co2–O15	85.3(3)
O6–Co1–N3	84.5(2)	O13–Co2–O14	91.9(3)
O8–Co1–N3	93.3(2)	O13–Co2–O15	90.7(3)
N1–Co1–N3	170.9(2)	O14–Co2–O15	175.1(4)

to the twofold axis. Three water solvate molecules are statistically disordered with the total positional occupancies of 0.5, one of which is also disordered over two sites in the ratio of 0.3:0.2. The O11 oxygen atom occupies a special position on the twofold axis (Fig. 2). The Co2–O bond distances differ significantly and are in the range of 1.949(9)–2.201(4) Å.

In the crystal of **CoL** there are numerous hydrogen bonding interactions with participation of water molecules. Details of the hydrogen bonds are listed in Table 2.

Table 2
Hydrogen bonds for **CoL**.

D–H···A	d(D–H) (Å)	d(H···A) (Å)	d(D···A) (Å)	∠ (DHA) (°)
O11–H11A···O7[a]	0.95	2.13	2.927(8)	141
O12–H12B···O17	0.90	1.92	2.765(13)	155
O12–H12C···O6[a]	0.90	1.85	2.718(10)	161
O13–H13A···O1	0.90	2.04	2.749(10)	134
O14–H14A···O19[b]	0.90	1.94	2.733(10)	147
O14–H14B···O14[a]	0.90	1.55	2.344(10)	146
O15–H15B···O17	0.90	2.13	2.639(11)	115
O16–H16D···O8[c]	0.93	2.37	3.058(6)	131
O16–H16D···O9[c]	0.93	2.10	2.973(6)	155
O16–H16E···O3[c]	0.93	2.13	2.973(6)	150
O16–H16E···O4[c]	0.93	2.33	2.949(6)	123
O17–H17D···O16	0.91	1.92	2.703(11)	143
O17–H17E···O18	0.91	2.02	2.868(13)	154
O18–H18A···O1[d]	0.91	2.23	3.060(10)	151
O18–H18B···O19[c]	0.91	2.12	2.822(13)	133
O18–H18B···O19′[c]	0.91	2.50	3.078(13)	122
O19–H19A···O7[e]	0.92	2.03	2.902(13)	158
O19–H19B···O18[f]	0.92	2.06	2.822(13)	139

Symmetry transformations used to generate equivalent atoms: (*a*) $x-y, -y, -z+2/3$; (b) $x-1, y-1, z$; (c) $-y+1, x-y, z+1/3$; (d) $y, x, -z+1$; (e) $-y+1, x-y+1, z+1/3$; (f) $-x+y+1, -x+1, z-1/3$

3.2. IR-spectroscopy

The IR spectra of **NaL** and **CoL** complex are presented in Fig 3a and b, respectively. Both spectra show a strong band at 1648 cm^{-1}, which is typical for Schiff-base ligands [35–37]. The bands in the **CoL** spectrum at 1533 and 1380 cm^{-1} are assigned to asymmetrical and symmetrical stretching C=O vibrations of carboxyl groups, and the great difference between them confirms the strong covalent binding between carboxyl groups and the cobalt ion [38], while in the **NaL** spectrum this difference is smaller, which is in good agreement with literature data [39]. The broad absorption band at 3376 cm^{-1} in the **CoL** spectrum can be attributed to free hydroxyl groups as well as to water coordinated to the cobalt ion [37,40]. The phenol ring skeleton vibrations appeared as shoulder at 1597 cm^{-1} and phenolic C–C and C–O vibrations are overlapped

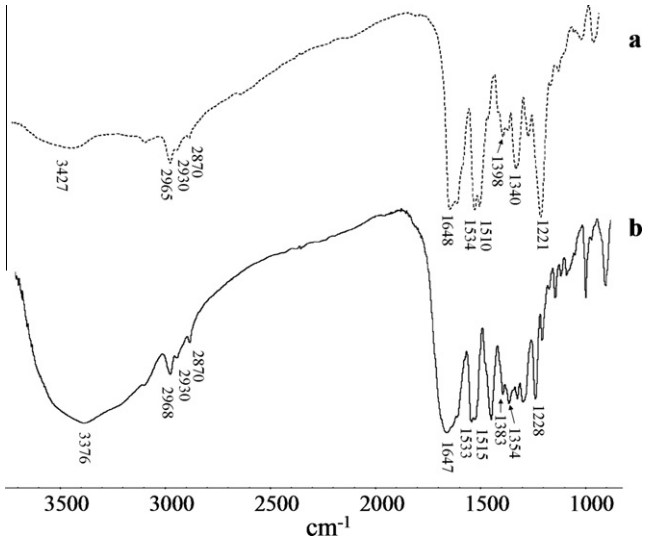

Fig. 3. IR spectra of **NaL** (a) and fresh **CoL** (b).

Table 3
XPS peaks of fresh **CoL** and of re-used **CoL**.

XPS peak		Co 2p3/2	Co 2p1/2	C 1s	O 1s	N 1s	Cl 2p
Binding energy (eV)	Fresh **CoL**	780.9	796.2	284.4	531.4	398.9	199.6
				287.1	533.5	404.9	
	Re-used **CoL**	780.7	796.5	284.3	531.3	399.0	199.8
				287.3	533.3	404.9	

to each other and cause a band at 1228 cm^{-1} [35,41], while in the spectrum of **NaL** very high intensity of the band at 1221 cm^{-1}, related to phenolic C–O vibrations, is due to the absence of bonding between phenolic OH group and cobalt ion. Two intense bands at 1515 and 1287 cm^{-1} for **CoL** and at 1510 and 1280 cm^{-1} for **NaL** are assigned to asymmetrical and symmetrical stretching N=O vibrations of nitro groups in the phenol ring [42]. The presence of amino acid in the sodium salt of ligand and the complex is confirmed by triple bands in the range 2840–2980 cm^{-1} due to the methyl C–H stretch [43].

Thus, composition and structure of the **CoL** complex, first synthesized in this work, were confirmed by XRD, elemental analysis and IR spectroscopy. It was found, that **CoL** can be represented as binuclear cobalt complex with one cobalt bonded to a Schiff base ligand and L-valine, and the other cobalt bonded to five water molecules and the oxygen atom in the carboxyl group of the amino acid.

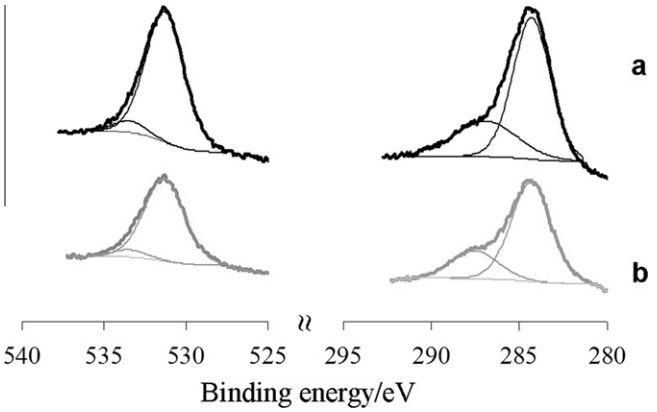

Fig. 5. XPS peaks in the O 1s and C 1s binding energy region for fresh **CoL** (a) and re-used **CoL** (b).

3.3. XPS

XPS measurements were carried out to determine the cobalt oxidation state in the surface region of the crystals and to compare fresh and re-used **CoL**.

The XPS results for the fresh **CoL** complex are given in Table 3 and Figs. 4 and 5. The N 1s spectrum of the complex has two components with an intensity ratio of 1:1 (Fig. 4). According to the literature [44,45], the first band at 398.9 eV can be attributed to azomethine nitrogen coordinated with the metal ion. The nitrogen in the NO_2 group, being more positive, has the higher binding energy (404.9 eV).

Two C 1s signals at 287.1 and 284.5 eV with an intensity ratio of 1:3 (Fig. 5) can be assigned to carbon connected with oxygen and nitrogen and carbon in phenol ring and aliphatic groups [45].

The oxygen atoms in **CoL** cause by a broad peak at 532 eV (FWHM – ca. 2.7 eV), which indicates the presence of different types of oxygen. Deconvolution of this broad peak leads to appearance of two bands at 533.5 and 531.5 eV (Fig. 5). The contribution at 531.5 eV can be attributed to oxygen in the nitro group, phenolic and carboxylic oxygen, while the band at 533.5 may arise from the C=O group coordinated with second cobalt ion, the positive shift contrary to literature data being due to the coordination with the second cobalt ion [46]. A Cl 2p signal can be attributed to the substituent at the benzene ring [47] (Fig. 4).

To determine the oxidation state of Co, the binding-energy difference between the $2p_{3/2}$ and $2p_{1/2}$ Co signals and the intensity of the satellite of the Co 2p signal is more reliable than the binding energy [48]. In **CoL** $\Delta(2p_{3/2} - 2p_{1/2})$ (15.23 eV) is close to that obtained for $Co(acac)_3$ [49] (Fig. 4). Also, the satellite peaks at the Co 2p signals are very small [50,51]. These results quite clearly demonstrate the predominance of Co 3^+ in the near-surface region.

In re-used **CoL**, the O 1s and C 1s signals are quite similar to the signals observed for fresh **CoL** (Fig. 5), while the intensity ratio of the N 1s signals has changed to 2.5:1 for amino and nitro group, which testifies a partial substitution of nitro groups in phenol ring (Fig. 5). This is possible with simultaneous partial substitution of chloride group also observed in XPS spectra (Fig. 4).

The $\Delta(2p_{3/2} - 2p_{1/2})$ binding energy difference for Co 2p increased from 15.23 eV (fresh **CoL**) to 15.85 eV (re-used **CoL**), indicating that cobalt was largely transformed from Co^{3+} to Co^{2+}. The broad satellite peaks observed for **CoL** after catalysis (Fig. 4), confirm this suggestion [50,51].

Thus, it was found, that the during catalytic experiment cobalt atoms in **CoL** complex partially changed the oxidation state from

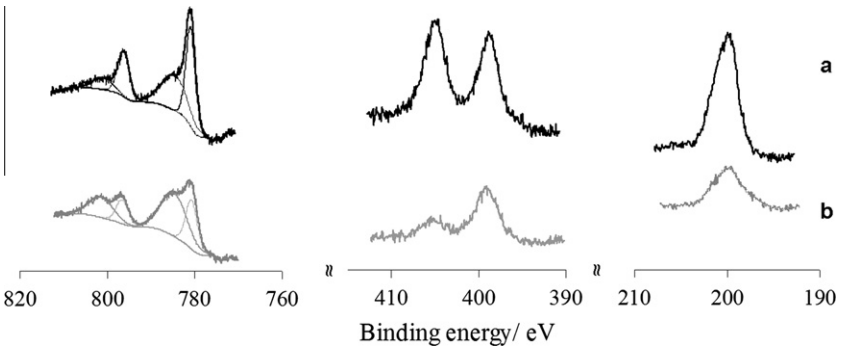

Fig. 4. XPS peaks (Co 2p, O 1s, N 1s and Cl 2p region) for fresh **CoL** (a) and re-used **CoL** (b).

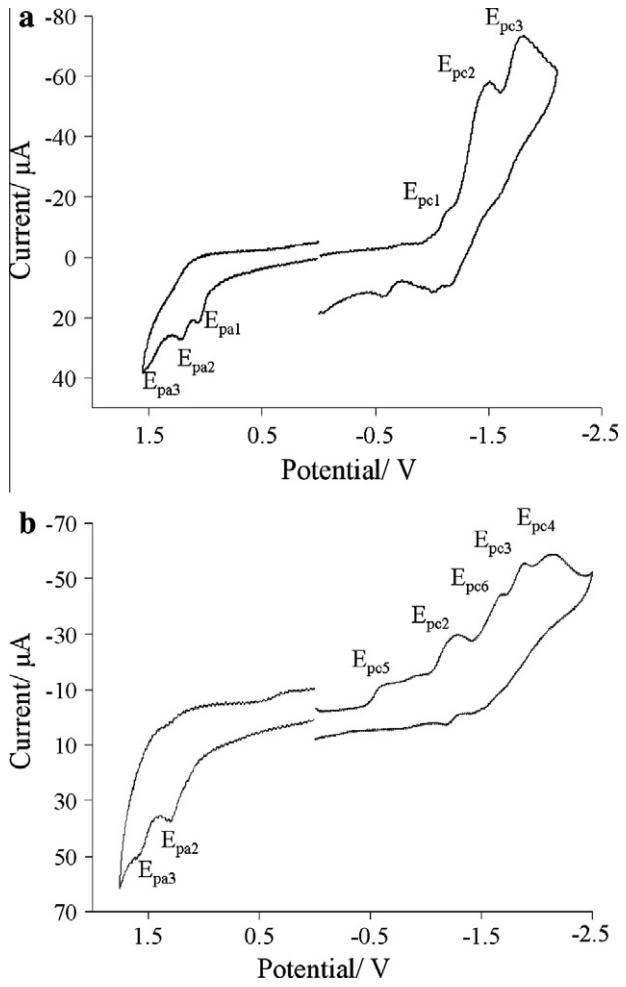

Fig. 6. Cyclic voltammograms of **NaL** (a); **CoL** (b) in DMF solution containing 0.1 M TBP. Scan rates = 0.200 V s^{-1}.

Co^{3+} to Co^{2+} because of a transformation of the Schiff base ligand with substitution of the nitro and chloride groups in the benzene ring.

3.4. Electrochemical studies

The electrochemical investigations of **CoL** and **NaL** were carried out to confirm the oxidation state of cobalt in the complex; the sodium salt of the ligand was used as a reference to determine the region of cobalt oxidation and reduction processes. Cyclic voltammograms (CV) obtained are shown in Fig. 6 and the electrochemical oxidation and reduction potentials are given in Table 4.

The sodium salt of ligand is electrochemically inactive in the range from −1 to +1 V. In the cathodic region of **NaL** CV, two irreversible peak are shown at $E_{pc2} = -1.48$ V and $E_{pc3} = -1.86$ V. Moreover, a low-intensity peak at $E_{pc1} = -1.11$ V indicates the adsorption of the initial complex on the electrode surface [52].

In addition to the above ligand-based processes, the **CoL** complex shows two irreversible reductions at $E_{pc5} = -0.64$ V and $E_{pc6} = -1.85$ V. The first two-electron irreversible reduction peak presumably corresponds to the reduction of two non-connected Co^{3+} ions to Co^{2+} [53,54], while irreversible one-electron reduction peak at −1.85 V can be attributed to the reduction of Co^{2+} to Co^{1+} [55,56]. The irreversible reduction of Co^{3+} to Co^{2+} proceeds by the mechanism ECE. Furthermore, the first ligand based reduction peak displaces in more positive direction in the CV of **CoL** because of the less ionic character of the bond between cobalt and the ligand in the complex than in the sodium salt of the ligand.

In the anodic region of CV of **CoL** only two oxidation peaks are present, the complex is oxidized at more positive potentials compared to the corresponding sodium salt of the ligand. An additional oxidation peak at $E_{pa1} = 1.00$ V in CV of **NaL** can be attributed to the Kolbe reaction [57], which is impossible in **CoL**.

3.5. Cyclohexane oxidation with air

The **CoL** complex was tested in the partial oxidation of cyclohexane with air to produce a mixture of CyOH and CyO. In addition to alcohol and ketone, CyOOH was formed, which is the evidence of the radical chain mechanism of CyH oxidation in the presence of the cobalt complex. Berezin and Denisov demonstrated, that such cobalt-salt based catalysts have three functions in alkane oxidation processes: an initiating function, an abscopal function and a products regulation function [58]. The initiation function is explained by reaction of Co^{3+} with alkane under formation of free radicals and Co^{2+}.

As reported on Fig. 7, cyclohexane oxidation without catalyst has a considerable induction period, corresponding to the initiation step shown in Eqs. (1)–(3).

$$RH + In^{\cdot} \rightarrow R^{\cdot} + In \quad (1)$$

$$R^{\cdot} + O_2 \rightarrow RO_2^{\cdot} \quad (2)$$

$$RO_2^{\cdot} + RH \rightarrow ROOH + R^{\cdot} \quad (3)$$

The end of the induction period corresponds to the accumulation of a significant amount of cyclohexyl hydroperoxide, which decomposes under formation of cyclohexanol and cyclohexanone (Fig. 7). The initiating function of **CoL** is clearly demonstrated by a considerable decrease of the induction period: CyH conversion reaches the maximum conversion (4.5%, limited by the amount of oxygen available) after 50 min, as compared with 240 min in the non-catalytic experiment.

The product selectivity as a function of reaction time is presented on Fig. 8. The amount of CyOOH decreases with reaction time due to the decomposition under formation of CyOH and CyO, and after 60 min the content of all products reaches a constant level. Cyclohexanol and cyclohexanone undergo further oxidation, forming a number of acids (butyric acid, adipic acid, hexanoic acid), which are unfavorable products. After 4 h the total selectivity for main products reaches 85%, with selectivity to cyclohexanol and cyclohexanone of 53% and 32%, respectively (Fig. 9). For comparison, the total selectivity for non-catalytic oxidation is only 74%, with 30% for cyclohexanol and 43% for cyclohexanone. Change of the CyOH/CyO ratio for catalytic and non-catalytic oxidation (1.65 and 0.68, respectively) is the confirmation of the product regulation function of **CoL**. In non-catalytic process there is also a large amount of unreacted cyclohexyl hydroperoxide in the

Table 4
Electrochemical data of **NaL** and fresh **CoL**[a].

Compound	E_{pc1}	E_{pc2}	E_{pc3}	E_{pc4}	E_{pc5}	E_{pc6}	E_{pa1}	E_{pa2}	E_{pa3}
NaL	−1.11	−1.48	−1.86	–	–	–	1.00	1.16	1.43
CoL	–	−1.36	−2.05	−2.36	−0.64	−1.85	–	1.23	1.52

[a] Potentials are vs. Ag/AgCl in 0.1 M, samples concentrations are 10^{-3} mol/l.

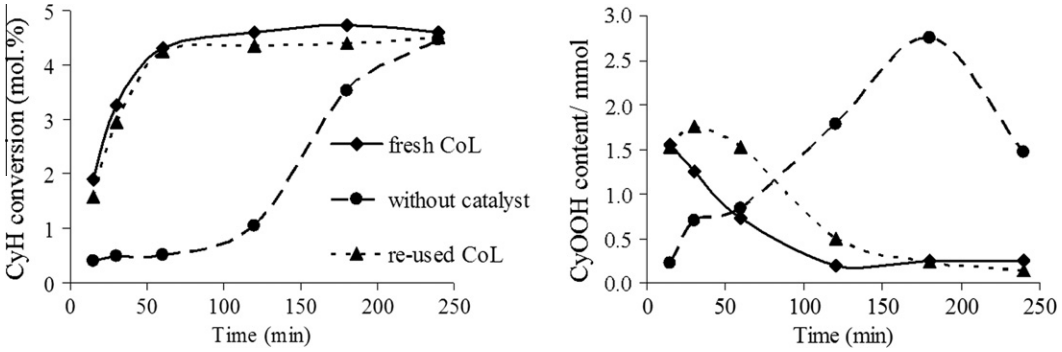

Fig. 7. CyH conversion and CyOOH content without catalyst, with fresh **CoL** and with re-used **CoL**. Cyclohexane (0.36 mol), toluene as internal standard (0.09 mol), catalyst (6.5×10^{-6} mol), 140 °C, 25 atm of air, stirrer.

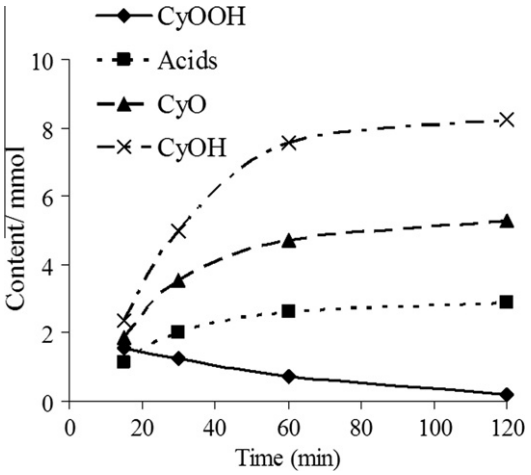

Fig. 8. Product selectivities on fresh **CoL** complex. Cyclohexane (0.36 mol), toluene as internal standard (0.09 mol), catalyst (6.5×10^{-6} mol), 140 °C, 25 atm of air, stirrer.

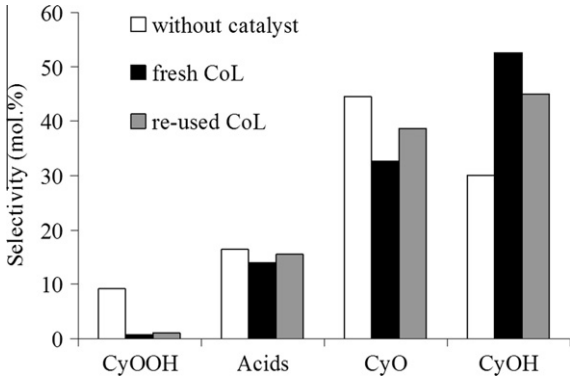

Fig. 9. Distribution of main products without catalyst, with fresh **CoL** and with re-used **CoL**. Cyclohexane (0.36 mol), toluene as internal standard (0.09 mol), catalyst (6.5×10^{-6} mol), 140 °C, 25 atm of air, stirrer, reaction time 4 h.

product mixture unlike in the **CoL** catalyzed reaction, which indicates that **CoL** also catalyzes the decomposition of cyclohexyl hydroperoxide by Haber–Weiss reactions (Eqs. (4) and (5)) [59].

$$ROOH + Co^{3+} \rightarrow ROO^{\cdot} + Co^{2+} + H^{+} \quad (4)$$

$$ROOH + Co^{2+} \rightarrow RO^{\cdot} + Co^{3+} + OH^{-} \quad (5)$$

The oxidation of Co^{2+} to Co^{3+}, which is not observed in the electrochemical investigation, takes place according the Eq. (5). This process is probably faster than the chemical reaction in an electrochemical cell.

The cyclohexane conversion on the re-used **CoL** develops very similar as on the fresh complex (Fig. 7), but the distribution of the main products differs. With re-used **CoL** the alcohol to ketone ratio is smaller (Fig. 9). This is due to partial transformation of Co^{3+} in the fresh complex to Co^{2+} in spent one (as was shown in Section 3.3), which leads to changes in the product regulation function of catalysts. At the same time, cyclohexane conversion and selectivities to the main products for **CoL** after catalysis are still higher, than obtained without catalyst or with catalysts on the basis of cobalt salts.

Since the CyH conversion and main products selectivities strongly depend on the type of the oxidant it is advisable to compare different catalysts using the same oxidant. Taking this into account, it is possible to compare the activity of **CoL** with Au/SBA-15 [60], which demonstrates selectivity of CyOH and CyO mixture about 73% with the time to reach 4% CyH conversion level about 90 min. Thus, the **CoL** is more active and selective catalyst for cyclohexane oxidation with air.

4. Conclusions

A new binuclear cobalt complex with a Schiff base ligand and an amino acid was synthesized and characterized by a number of physical measurements. Structure, composition, oxidative properties of complex were fully investigated and the presence of cobalt in the oxidation state 3+ was shown in this complex.

Fresh and used complexes were tested in partial cyclohexane oxidation with air and high activity and selectivity for cyclohexanol and cyclohexanone were observed. A radical chain mechanism of cyclohexane oxidation over the **CoL** complex was verified by detection of cyclohexyl hydroperoxide as intermediate reaction product. It was clearly demonstrated, that cobalt in oxidation state 3+ is more preferable for catalytic cyclohexane oxidation. Transformation of Co^{3+} to Co^{2+} leads to a slight decrease in catalyst activity and changes in main product distribution.

Acknowledgments

L.I. Rodionova thanks the German Academic Exchange Service (DAAD) for a Leonhard Euler Grant.

Appendix A. Supplementary material

CCDC 855626 contains the supplementary crystallographic data for this paper. These data can be obtained free of charge from The

Cambridge Crystallographic Data Centre via www.ccdc.cam.ac.uk/data_request/cif.

References

[1] A.K. Suresh, M.M. Sharma, T. Sridhar, Ind. Eng. Chem. Res. 39 (2000) 3958.
[2] J.M. Brégeault, Dalton Trans. (2003) 3289.
[3] M.T. Musser, Ullmann's Encyclopedia of Industrial Chemistry, fifth ed., Wiley-VCH, Weinheim, 2007. vol. 11, pp. 51–52.
[4] U. Schuchardt, D. Cardoso, R. Sercheli, R. Pereira, R.S. da Cruz, M.C. Guerreiro, D. Mandelli, E.V. Spinacé, E.L. Pires, Appl. Catal. A 211 (2001) 1.
[5] C. Guo, M. Chu, Q. Liu, Y. Liu, D. Guo, X. Liu, Appl. Catal. A 246 (2003) 303.
[6] B. Qiu, J. Gui, X. Zhang, D. Liu, Z. Sun, Pet. Sci. Technol. 24 (2006) 1331.
[7] J. Tong, L. Boc, Z. Li, Z. Lei, C. Xia, J. Mol. Catal. A: Chem. 307 (2009) 58.
[8] M. Salavati-Niasari, Z. Salimi, M. Bazarganipour, F. Davar, Inorg. Chim. Acta 362 (2009) 3715.
[9] M. Dolaz, V. McKee, S. Uruş, N. Demir, A.E. Sabik, A. Gölcü, M. Tümer, Spectrochim. Acta, Part A 76 (2010) 174.
[10] F.A. Chavez, J.M. Rowland, M.M. Olmstead, P.K. Mascharak, J. Am. Chem. Soc. 120 (1998) 9015.
[11] J.T. Groves, J. Inorg. Biochem. 100 (2006) 434.
[12] G.C. Silva, G.L. Parrilha, N.M.F. Carvalho, V. Drago, C. Fernandes, A. Horn Jr., O.A.C. Antunes, Catal. Today 133–135 (2008) 684.
[13] M.C. Esmelindro, E.G. Oestreicher, H. Márquez-Alvarez, C. Dariva, S.M.S. Egues, C. Fernandes, A.J. Bortoluzzi, V. Drago, O.A.C. Antunes, J. Inorg. Biochem. 99 (2005) 2054.
[14] C. Guo, X. Liu, Q. Liu, Y. Liu, M. Chu, W. Lin, J. Porphyrins Phthalocyanines 13 (2009) 1250.
[15] A. Hussain, R.S. Shukla, R.B. Thorat, H.J. Padhiyar, K.N. Bhatt, J. Mol. Catal. A: Chem. 193 (2003) 1.
[16] L. Casella, M. Gullotti, Inorg. Chem. 25 (9) (1986) 1293.
[17] G.M. Sheldrick, SADABS, v 2.03, Bruker/Siemens Area Detector Absorption Correction Program, Bruker AXS, Madison, Wisconsin, 2003.
[18] G.M. Sheldrick, Acta Crystallogr., Sect. A 64 (2008) 112.
[19] L.I. Kuznetsova, L.G. Detusheva, N.I. Kuznetsova, V.K. Duplyakin, V.A. Licholobov, Kinet. Catal. 49 (5) (2008) 644.
[20] A.M. Abdel-Mawgoud, S.A. El-Gyar, M.M.A. Hamed, Synth. React. Inorg. Met.-Org. Chem. 21 (1991) 1061.
[21] Y.N. Belokon, V.I. Maleev, I.L. Malifanov, T.F. Savelieva, N.S. Ikonnikov, A.G. Bulychev, D.L. Usanov, D.A. Kataev, M. North, Russ. Chem. Bull. 55 (2006) 821.
[22] V.I. Maleev et al., Russ. Chem. Bull. 59 (2010) 598.
[23] V.B. Badwaik, R.D. Deshmukh, A.S. Aswar, Russ. J. Coord. Chem. 35 (2009) 247.
[24] M.S. Islam, M. Begum, H.N. Roy, Synth. React. Inorg. Met.-Org. Chem. 25 (1995) 293.
[25] P.K. Panchal, D.H. Patel, M.N. Patel, Synth. React. Inorg. Met.-Org. Chem. 34 (2004) 1223.
[26] P.K. Panchal, M.N. Patel, Synth. React. Inorg. Met.-Org. Chem. 34 (2004) 1277.
[27] H.M. Parekh, S.R. Mehta, M.N. Patel, Russ. J. Inorg. Chem. (Zh. Neorg. Khim.) 51 (2006) 67.
[28] H.M. Parekh, M.N. Patel, Russ. J. Coord. Chem. 32 (2006) 431.
[29] N. Thankarajan, K. Mohanan, Indian J. Chem., Sect. A 27 (1988) 360.
[30] W. Zishen, G. Ziqi, Y. Zhenhuan, Synth. React. Inorg. Met.-Org. Chem. 20 (1990) 335.
[31] Y.N. Belokon, Pure Appl. Chem. 64 (12) (1992) 1917.
[32] Y.N. Belokon, L.K. Pritula, V.I. Tararov, V.I. Bakhmutov, Y.T. Struchkov, T.V. Timofeeva, V.M. Belikov, J. Chem. Soc., Dalton Trans. 6 (1990) 1873.
[33] L.R. Nassimbeni, G.C. Percy, A.L. Rodgers, Acta Crystallogr., Sect. B: Struct. Sci. 32 (1976) 1252.
[34] J. Han, Y.H. Xing, F.Y. Bai, X.J. Zhang, X.Q. Zeng, M.F. Ge, J. Coord. Chem. 62 (2009) 2719.
[35] B.A. El-Sayed, M.M. Abo Aly, A.A.A. Emara, S.M.E. Khail, Vib. Spectrosc. 30 (2002) 93.
[36] G. Leniec, S.M. Kaczmarek, J. Typek, B. Ko1odziej, E. Grech, W. Schilf, Solid State Sci. 9 (2007) 267.
[37] J. Costa Pessoa, I. Cavaco, I. Correia, M.T. Duarte, R.D. Gillard, R.T. Henriques, F.J. Higes, C. Madeira, I. Tomaz, Inorg. Chim. Acta 293 (1999) 1.
[38] K. Nakamoto, Infrared and Raman Spectra of Inorganic and Coordination Compounds, fourth ed., Wiley, New York, 1986. pp. 259–270.
[39] B.E. Zaycev, Spectrochemistry of Coordination Compounds, RUDN, Moscow, 1991. pp. 151–155 (in Russian).
[40] A.A.A. Emara, A.A.A. Abou-Hussen, Spectrochim. Acta, Part A 64 (2006) 1010.
[41] H. Eshtiagh-Hosseini, M.R. Housaindokhta, S. Ali Beyramabadi, S. Beheshti, A.A. Esmaeili, M.J. Khoshkholghb, A. Morsali, Spectrochim. Acta, Part A 71 (2008) 1341.
[42] K. Nakanishi, Infrared Absorption Spectroscopy, Holden-Day, Inc., San Francisco and Nankodo Company Limited, Tokyo, 1962. pp. 61–67.
[43] D.M. Boghaei, M. Gharagozlou, Spectrochim. Acta, Part A 67 (2007) 944.
[44] K. Burger, H. Ebel, M. Ebel, C. Várhelyi, Inorg. Chim. Acta 88 (1984) L11.
[45] D. Atzei, D. de Filippo, A. Rossi, R. Caminiti, Spectrochim Acta 49 (12) (1993) 1779.
[46] K.B. Yatsimirskii, V.V. Nemoskalenko, V.G. Aleshin, Yu.I. Bratushko, E.P. Moiseenko, Chem. Phys. Lett. 52 (3) (1977) 481.
[47] D.T. Clark, D. Kilcast, D.B. Adams, W.K.R. Musgrave, J. Electron Spectrosc. Relat. Phenom. 6 (1975) 117.
[48] Y. Okamoto, H. Nakano, T. Imanaka, S. Teranishi, Bull. Chem. Soc. Jpn. 48 (1975) 1163.
[49] D. Atzei, A. Rossi, C. Sadun, Spectrochim. Acta, Part A 56 (2000) 1875.
[50] D. Briggs, V.A. Gibson, Chem. Phys. Lett. 25 (4) (1974) 493.
[51] T. Ivanova, A. Naumkin, A. Sidorov, I. Eremenko, M. Kiskin, J. Electron Spectrosc. Relat. Phenom. 156–158 (2007) 200.
[52] A.A. Moiseeva, S.V. Stepanov, K.P. Butin, O.B. Jidkova, O.M. Khitrova, V.I. Bregadze, Russ. Chem. Bull. 9 (2003) 1877.
[53] A. Böttcher, T. Takeuchi, K.I. Hardcastle, T.J. Meade, H.B. Gray, D. Cwikel, M. Kapon, Z. Dori, Inorg. Chem. 36 (1997) 2498.
[54] R. Bikas, H.H. Monfared, T. Lis, M. Siczek, Inorg. Chem. Commun. 15 (2012) 151.
[55] S. Meghdadi, M. Amirnasr, K. Mereiter, H. Molaee, A. Amiri, Polyhedron 30 (2011) 1651.
[56] J. Asseraf, F. Bedioui, O. Reyes, Y. Robin, J. Devynck, C. Bied-Charreton, J. Electroanal. Chem. 170 (1983) 255.
[57] C.K. Mann, K.K. Barnes, Electrochemical Reaction in Nonaqueous Systems, Marcel Dekker, New York, 1970. pp. 136–138.
[58] I.V. Berezin, E.T. Denisov, The Oxidation of Cyclohexane, Pergamon Press, New York, 1996. pp. 175–190.
[59] F. Haber, J. Weiss, Naturwissenschaften 20 (1932) 948.
[60] B.P.C. Hereijgers, B.M. Weckhuysen, J. Catal. 270 (2010) 16.